Sharp tunable optical filters based on the polarization attributes of stimulated Brillouin scattering

Assaf Wise,[1,*] Moshe Tur[1], and Avi Zadok[2]

[1]*Faculty of Engineering, Tel-Aviv University, Tel-Aviv 69978, Israel*
[2]*School of Engineering, Bar-Ilan University, Ramat-Gan 52900, Israel*
**assafwise@yahoo.com*

Abstract: Sharp and highly-selective tunable optical band-pass filters, based on stimulated Brillouin scattering (SBS) amplification in standard fibers, are described and demonstrated. Polarization pulling of the SBS-amplified signal wave is used to increase the selectivity of the filters to 30 dB. Pump broadening via synthesized direct modulation was used to provide a tunable, sharp and uniform amplification window: Pass-band widths of 700 MHz at half maximum and 1GHz at the −20dB points were obtained. The central frequency, bandwidth and shape of the filter can be arbitrarily set. Compared with scalar SBS-based filters, the polarization-enhanced design provides a higher selectivity and an elevated depletion threshold.

OCIS codes: (190.0190) Nonlinear optics; (290.5830) Scattering, Brillouin; (060.4370) Nonlinear Optics, Fibers

References and links

1. G. P. Agrawal, *Fiber-Optic communication systems*, third edition, (Wiley, 2002), Chapter 8, pp.330–403.
2. J. Capmany, B. Ortega, D. Pastor, and S. Sales, "Discrete-time optical processing of microwave signals," J. Lightwave Technol. **23**(2), 702–723 (2005).
3. T. A. Strasser and T. Erdogan, "Fiber grating devices in high performance optical communication systems," chapter 10 of Optical fiber telecommunications IVA – components. I. P. Kaminow, and T. Li (editors), San Diego, CA: Academic press, 2002.
4. A. Yariv, chapter 4 in Optoelectronics, pp. 110–116, Orlando FL: Saunders College Publishing, 4th Edition, 1991.
5. C. R. Doerr, "Planar lightwave devices for WDM," chapter 9 of Optical fiber telecommunications IVA – components. I. P. Kaminow, and T. Li (editors), San Diego, CA: Academic press, 2002.
6. T. Tanemura, Y. Takushima, and K. Kikuchi, "Narrowband optical filter, with a variable transmission spectrum, using stimulated Brillouin scattering in optical fiber," Opt. Lett. **27**(17), 1552–1554 (2002).
7. A. Zadok, A. Eyal, and M. Tur, "GHz-wide optically reconfigurable filters using stimulated Brillouin scattering," J. Lightwave Technol. **25**(8), 2168–2174 (2007).
8. R. W. Boyd, *Nonlinear Optics,* third edition, (Academic Press, 2008).
9. M. Nikles, L. Thévenaz, and P. Robert, "Brillouin gain spectrum characterization in single-mode optical fibers," J. Lightwave Technol. **15**(10), 1842–1851 (1997).
10. J. C. Yong, L. Thévenaz, and B. Y. Kim, "Brillouin fiber laser pumped by a DFB laser diode," J. Lightwave Technol. **21**(2), 546–554 (2003).
11. A. Loayssa and F. J. Lahoz, "Broadband RF photonic phase shifter based on stimulated Brillouin scattering and single side-band modulation," IEEE Photon. Technol. Lett. **18**(1), 208–210 (2006).
12. A. Loayssa, J. Capmany, M. Sagues, and J. Mora, "Demonstration of incoherent microwave photonic filters with all-optical complex coefficients," IEEE Photon. Technol. Lett. **18**(16), 1744–1746 (2006).
13. Z. Zhu, D. J. Gauthier, and R. W. Boyd, "Stored light in an optical fiber via stimulated Brillouin scattering," Science **318**(5857), 1748–1750 (2007).
14. L. Thevenaz, "Slow and Fast Light Using Stimulated Brillouin Scattering: A Highly Flexible Approach," in *Slow Light – Science and Applications,* J. B. Khurgin and R. S. Tucker Eds. (CRC press, 2009), pp. 173–193.
15. A. Zadok, A. Eyal, and M. Tur, "Stimulated Brillouin scattering slow light in optical fibers," Appl. Opt. **50**(25), E38–E49 (2011).
16. A. Zadok, E. Zilka, A. Eyal, L. Thévenaz, and M. Tur, "Vector analysis of stimulated Brillouin scattering amplification in standard single-mode fibers," Opt. Express **16**(26), 21692–21707 (2008).

#152142 - $15.00 USD Received 1 Aug 2011; revised 31 Aug 2011; accepted 1 Sep 2011; published 21 Oct 2011

17. A. Zadok, S. Chin, L. Thévenaz, E. Zilka, A. Eyal, and M. Tur, "Polarization-induced distortion in stimulated Brillouin scattering slow-light systems," Opt. Lett. **34**(16), 2530–2532 (2009).
18. M. Wuilpart, "Distributed measurement of polarization properties in single-mode optical fibres using a reflectometry technique", Ph.D. Thesis, Faculte Polytechnique de Mons (2003).
19. H. Sunnerud, C. Xie, M. Karlsson, R. Samuelsson, and P. Andrekson, "A comparison between different PMD compensation techniques," J. Lightwave Technol. **20**(3), 368–378 (2002).
20. C. Y. Wong, R. S. Cheng, K. B. Letaief, and R. D. Murch, "Multiuser OFDM with adaptive subcarrier, bit, and power allocation," IEEE J. Sel. Areas Comm. **17**(10), 1747–1758 (1999).
21. M. Sagues and A. Loayssa, "Orthogonally polarized optical single sideband modulation for microwave photonics processing using stimulated Brillouin scattering," Opt. Express **18**(22), 22906–22914 (2010).

1. Introduction

Optical tunable filters are widely used for channel selection within dense wavelength division multiplexing (DWDM) telecommunication networks [1], for the reduction of amplified spontaneous emission noise following optical amplification [1], as well as in microwave photonic processing setups [2]. The primary figures of merit for tunable optical filters are low insertion loss, sharp transition between the pass-band and stop-bands, high side-lobe suppression, and a broad tuning range. Several mature technologies are available for the realization of passive tunable optical filters, such as fiber Bragg gratings (FBGs) [3], Fabry-Perot etalons (FPs) [4], Mach-Zehnder interferometers and ring resonators in planar light-guide circuits (PLCs) [5]. In such passive filters the bandwidth and spectral transmission shape are typically fixed. In contrast, active tunable optical filters allow for adjusting not only the transmission wavelength, but also the width and shape of the pass-band as well. In addition, active filters may amplify the signal within the frequency range of choice.

Active tunable optical filters have been previously proposed and demonstrated based on stimulated Brillouin scattering (SBS) in standard optical fibers [6,7]. SBS requires the lowest activation power of all non-linear effects in silica optical fibers. In SBS, a strong pump wave and a typically weak, counter-propagating signal wave optically interfere to generate, through electrostriction, a traveling longitudinal acoustic wave. The acoustic wave, in turn, couples these optical waves to each other [8]. The SBS interaction is efficient only when the difference between the optical frequencies of the pump and signal waves is very close (within a few tens of MHz) to a fiber-dependent parameter, the Brillouin shift Ω_B, which is on the order of $2\pi \cdot 11 \cdot 10^9$ [rad/sec] in silica fibers at room temperature and at telecommunication wavelengths [8]. An input signal whose frequency is Ω_B lower than that of the pump ('Stokes wave'), experiences SBS amplification. SBS has found numerous applications, including distributed sensing of temperature and strain [9], fiber lasers [10], optical processing of high frequency microwave signals [11,12] and even optical memories [13]. Over the last six years SBS has been highlighted as the preferred mechanism in many demonstrations of variable group delay setups [14,15], often referred to as slow and fast light.

In previous demonstrations, selective SBS amplification with an arbitrary central frequency and a sharp pass-band of up to 2.5 GHz width was demonstrated [6,7]. The amplification bandwidth was broadened using pump wave synthesized modulation [7]. The central frequency, bandwidth and gain selectivity of the filters were all separately tunable. However, the selective amplification of the filters was limited by the onset of the amplified spontaneous emission that is associated with SBS (SBS-ASE), and use of the filters was restricted to relatively weak signal power levels by pump depletion. In this paper, we enhance the spectral selectivity of SBS tunable filters, and elevate their depletion threshold. The solution path relies on the polarization attributes of SBS in standard, weakly birefringent fibers. A vector analysis of SBS reveals that the state of polarization (SOP) of the amplified signal is drawn towards a particular state, which is governed by the SOP of the pump [16]. That particular state could be made different from the output polarization of unamplified, out-of-band signal components, unaffected by SBS. Based on this principle, the filters described in this work combine a relatively modest SBS amplification within the filter pass-band,

#152142 - $15.00 USD Received 1 Aug 2011; revised 31 Aug 2011; accepted 1 Sep 2011; published 21 Oct 2011

together with polarization discrimination for out-of-band rejection. A 700 MHz-wide, sharp band-pass filter with 30 dB selectivity is demonstrated experimentally.

2. Principle of operation

Consider the Jones vector $\vec{E}_{sig}(z)$ of a monochromatic signal of optical frequency ω_{sig}, entering the fiber at $z = 0$, where z denotes the position along a fiber of length L. A broadened, counter-propagating pump wave of power spectral density (PSD) $P(\omega_p)$ enters the fiber at $z = L$. We denote the unit Jones vector of the pump wave as $\hat{e}_{pump}(z)$. The same {x, y} coordinate axes are used for both Jones vectors (as in [16]). We neglect linear losses, as well as polarization mode dispersion effects within the spectral range of $\Omega_B \sim 2\pi \cdot 11 \cdot 10^9$ rad/sec. The propagation equation of $\vec{E}_{sig}(z)$ in the undepleted pump regime is given by Eq. (1) [16]:

$$\frac{d\vec{E}_{sig}\left(z,\omega_{sig}\right)}{dz} = \left\{ \frac{d\mathbf{T}(z)}{dz}\mathbf{T}^{\dagger}(z) + \frac{g(\omega_{sig})}{2}\left[\hat{e}_{pump}(z)\hat{e}^{\dagger}_{pump}(z)\right]\right\}\vec{E}_{sig}\left(z,\omega_{sig}\right) \tag{1}$$

$\mathbf{T}(z)$ is the Jones matrix, which describes the linear signal propagation along the fiber up to point z, and $g(\omega_{sig})$ (in units of m^{-1}) is given by a convolution of the pump PSD with the inherent Lorentzian line shape of the SBS process [14,15]:

$$g\left(\omega_{sig}\right) = \int \frac{\frac{1}{2}\gamma_0 P(\omega_p)}{1 - j2\left(\omega_p - \omega_{sig} - \Omega_B\right)/\Gamma_B} d\omega_p \,. \tag{2}$$

Here $\Gamma_B \sim 2\pi \cdot 30 \cdot 10^6$ rad/sec is the SBS linewidth, and γ_0 is the SBS gain coefficient in units of $[W \cdot m]^{-1}$. The evolution of the counter-propagating, undepleted pump is governed by birefringence alone:

$$\hat{e}_{pump}(0) = \mathbf{T}^{T}(z)\hat{e}_{pump}(z) \rightarrow \hat{e}_{pump}(z) = \mathbf{T}^{*}(z)\hat{e}_{pump}(0) \tag{3}$$

where the superscript T stands for the transpose operation, and $\mathrm{inv}\left[\mathbf{T}^{T}(z)\right] = \mathbf{T}^{*}(z)$. Zadok *et al.* [16] have shown that the SBS amplification process in a birefringent fiber is characterized by maximum and minimum values of the signal amplitude gain, $G_{\max}(\omega_{sig})$ and $G_{\min}(\omega_{sig})$, respectively. The two gain values are complex, and they vary with the signal frequency. For the broadened, uniform $P(\omega_p)$ used in this work, the absolute values of $G_{\max}$ and $G_{\min}$ become nearly frequency-independent within the amplification bandwidth [14,15], (see Eq. (2). The maximum and minimum gain values are associated with a pair of orthogonal SOPs of the signal [16]. We denote the unit Jones vectors of these SOPs at the signal input end of the fiber as $\hat{e}_{sig}^{in\,max}$ and $\hat{e}_{sig}^{in\,min}$ respectively. The two extreme gain values are also associated with a pair of orthogonal SOPs of the signal output: $\hat{e}_{sig}^{out\,min}$ and $\hat{e}_{sig}^{out\,max}$. Both the input and the output pairs of SOPs were shown to be nearly frequency independent within the amplification bandwidth [17]. In sufficiently long, standards fibers, being weakly and randomly birefringent, the signal SOPs associated with maximum and minimum SBS amplification are related to those of the pump wave by [16]:

$$\hat{e}_{sig}^{in\,\max} = \hat{e}^{*}_{pump}(z=0); \quad \hat{e}_{sig}^{in\,\min} = \hat{e}^{*\perp}_{pump}(z=0) \tag{4}$$

$$\hat{e}_{sig}^{out\,\max} = \hat{e}^{*}_{pump}(z=L); \quad \hat{e}_{sig}^{out\,\min} = \hat{e}^{*\perp}_{pump}(z=L) \tag{5}$$

#152142 - $15.00 USD Received 1 Aug 2011; revised 31 Aug 2011; accepted 1 Sep 2011; published 21 Oct 2011

In Eq. (4) and (5), the superscript $*\perp$ denotes the orthogonal of the conjugate. Based on Eqs. (3-5) and the fact that $\left[\mathbf{T}^T(z)\right]^* = \mathrm{inv}\left[\mathbf{T}(z)\right]$, we find that the signal SOPs of maximum and minimum amplification at the fiber output are simply related to the corresponding input states by the birefringence matrix $\mathbf{T}(L)$:

$$\hat{e}_{sig}^{out\ \max} = \mathbf{T}(L)\hat{e}_{sig}^{in\ \max};\ \hat{e}_{sig}^{out\ \min} = \mathbf{T}(L)\hat{e}_{sig}^{in\ \min} \tag{6}$$

For low pump power values, the integrated impact of the Brillouin amplification almost solely depends on the relative orientations of the pump and signal SOP's along the fiber, as determined by the fiber birefringence. Hence, it is not surprising that the relationships of Eq. (6) do not depend on the Brillouin interaction. Yet, it is interesting to note that both numerically and experimentally, Eqs. (4-6) also hold, at least approximately, even for strong pumps and considerable Brillouin gains [16].

An input signal of arbitrary SOP can be decomposed along the basis of $\hat{e}_{sig}^{in\ max}$ and $\hat{e}_{sig}^{in\ min}$:

$$\vec{E}_{sig}(0) = a\hat{e}_{sig}^{in\ \max} + b\,\hat{e}_{sig}^{in\ \min}. \tag{7}$$

Following SBS amplification, the output signal vector becomes:

$$\vec{E}_{sig}^{SBS}(L) = aG_{\max}\cdot\hat{e}_{sig}^{out\ max} + bG_{\min}\cdot\hat{e}_{sig}^{out\ min}. \tag{8}$$

On the other hand, if the signal wave is subject to birefringence alone, the output vector is instead given by:

$$\vec{E}_{sig}^{biref}(L) = a\hat{e}_{sig}^{out\ max} + b\hat{e}_{sig}^{out\ min}. \tag{9}$$

For long enough [16], randomly and weakly birefringent fibers, the expected magnitudes of the maximum and minimum amplification are $|G_{\max}|^2 = \exp\left[\frac{2}{3}g(\omega_{sig})L\right]$ and $|G_{\min}|^2 = \exp\left[\frac{1}{3}g(\omega_{sig})L\right] = \sqrt{|G_{\max}|^2}$ [16]. For a sufficiently strong pump $|G_{\max}| >> |G_{\min}|$, and unless *a* is vanishingly small, Eq. (8) describes *polarization pulling* of the output probe wave towards a particular state, $\hat{e}_{sig}^{out\ max}$, which is determined by the pump polarization. The effectiveness of the pulling is governed by the ratio $|G_{\max}|/|G_{\min}|$. Equations (8) and (9) also show that SBS introduces a difference between the output SOP of amplified signal components, for which $g(\omega_{sig})$ is significant, and that of unamplified components, for which $g(\omega_{sig})$ is negligible. It is therefore possible to further discriminate between amplified and unamplified spectral components of a broadband signal wave, using a properly aligned polarizer.

Let $\hat{e}_{pol}$ denote the state of a polarizer placed at the signal output, $z = L$:

$$\hat{e}_{pol}(L) = p_{\max}\hat{e}_{sig}^{out\ max} + p_{\min}\hat{e}_{sig}^{out\ min}, \tag{10}$$

where $p_{\max,\min}$ are the projections of $\hat{e}_{pol}$ onto $\hat{e}_{sig}^{out\ max}$ and $\hat{e}_{sig}^{out\ min}$, respectively. At the polarizer output, the amplitude of an out-of-band, unamplified signal component is given by:

$$A_{sig}^{biref} = a\left(\hat{e}_{pol}^{\dagger}\cdot\hat{e}_{sig}^{out\ max}\right) + b\left(\hat{e}_{pol}^{\dagger}\cdot\hat{e}_{sig}^{out\ min}\right) = ap_{\max}^* + bp_{\min}^*. \tag{11}$$

#152142 - $15.00 USD Received 1 Aug 2011; revised 31 Aug 2011; accepted 1 Sep 2011; published 21 Oct 2011

With proper alignment of the output polarizer, A_{sig}^{biref} can be set to zero, signifying the (theoretical) complete rejection of out-of-band components. On the other hand, the amplitude of an SBS-amplified signal component at the polarizer output is:

$$\begin{aligned} A_{sig}^{SBS} &= aG_{\max}\left(\hat{e}_{pol}^{\dagger}\cdot\hat{e}_{sig}^{out\,max}\right)+bG_{\min}\left(\hat{e}_{pol}^{\dagger}\cdot\hat{e}_{sig}^{out\,min}\right)=aG_{\max}p_{\max}^{*}+bG_{\min}p_{\min}^{*} \\ &= ap_{\max}^{*}\left(G_{\max}-G_{\min}\right) \end{aligned} \tag{12}$$

The final equality in Eq. (12) is met when Eq. (11) is set to zero. Due to the differential gain of SBS, in-band components are retained and even amplified.

To calculate the SBS gain of the signal components we assume the signal input to be of unity power ($|a|^2+|b|^2=1$) so that:

$$In-band\ \ Gain=\left|A_{sig}^{SBS}\right|^2_{|a|^2+|b|^2=1}=\left|ap_{\max}^{*}\right|^2\left|G_{\max}-G_{\min}\right|^2\xrightarrow[G_{\max}>>G_{\min}]{}\left|ap_{\max}^{*}\right|^2\left|G_{\max}\right|^2 \tag{13}$$

Subject to the constraint of complete out-of-band rejection ($A_{sig}^{biref}=0$ in Eq. (11)) together with $|p_{\max}|^2+|p_{\min}|^2=1$, it is easy to show that this in-band SBS gain can become as high as $0.25|G_{\max}|^2$, provided: $|a|^2=|p_{\max}|^2=0.5$. Thus, the amplification of the polarization-assisted SBS process, at the high pump power limit, is only 6dB lower than that of a corresponding scalar process, when the latter is aligned for maximum gain. However, while polarization discrimination can achieve very high rejection (theoretically infinite) for the unamplified out-of-band components, the power transfer for these components in the scalar process is unity. We conclude that the polarization discrimination filtering proposed in this work can achieve much higher selectivity than its scalar counterpart.

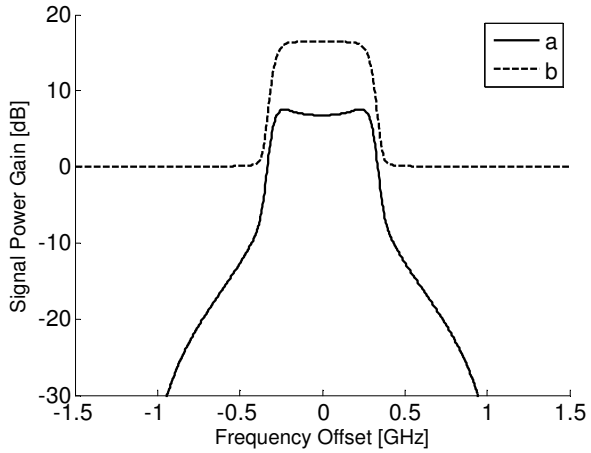

Fig. 1. Simulation results for the signal power gain at the output of an SBS amplification process, using a 3.6 km-long highly nonlinear fiber (HNLF) and a 0.7 GHz-wide, 13.5 dBm pump. The pump is assumed to be undepleted. In the lower curve (a), the input signal's SOP was chosen with equal projections on the states of maximum and minimum SBS amplification ($a=b=1/\sqrt{2}$, see text), and an output polarizer was aligned for maximal rejection of unamplified signal components ($p_{\max,\min}=\pm 1/\sqrt{2}$, see text). The upper curve (b) shows the corresponding power gain with no output polarizer, and with the input signal SOP aligned for maximum amplification (a = 1).

#152142 - $15.00 USD Received 1 Aug 2011; revised 31 Aug 2011; accepted 1 Sep 2011; published 21 Oct 2011

Figure 1 presents simulation results of the relative optical power transmission of the signal wave, as a function of the frequency offset from the pass-band center. In the simulations, Eq. (1) and (3) were directly integrated. A 3.5 km-long highly non-linear fiber (HNLF) with an SBS gain coefficient γ_0 = 2.9 [W·m]$^{-1}$ was used. The fiber was simulated as 1000 cascaded birefringent media that are randomly oriented, with a polarization beat length of 40 m and a polarization coupling length of 10 m [16,18]. The pump power was set to 13.5 dBm, and its PSD was uniform within a 0.7 GHz-wide region. The pump was assumed to be undepleted. Curve 1(b) shows the signal power gain for an SBS process with no output polarizer, and with the signal input SOP aligned for maximum amplification (a = 1). A filtering selectivity of $|G_{\max}|^2$ = 16.5 dB is obtained. In curve (a), the signal input SOP was chosen so that $a = b = 1/\sqrt{2}$, and an output polarizer was aligned to $p_{\max,\min} = \pm 1/\sqrt{2}$. The in-band amplification of the polarization-assisted filter was lowered by 10 dB, in agreement with the prediction of Eq. (13), where for the specific, rather modest pump power, $G_{\min}$ cannot be ignored and $|G_{\max} - G_{\min}|^2$ must be used instead of $|G_{\max}|^2$. However, the polarizer helps to significantly attenuate the out-of-band components so that the filtering selectivity is much improved. Two observations to be noted in Fig. 1(a): (i) The slightly larger amplification towards the pass-band edges originates from the complex nature $G_{\max}$ and $G_{\min}$: while both are real numbers in the band center, they have different phases at the edges, resulting in somewhat higher values for $|G_{\max} - G_{\min}|^2$; (ii) The gradual transition between the pass-band and stop-bands is due to the convolution form of $g(\omega_{sig})$, (Eq. (2). Lastly, the lower in-band amplification is expected to defer the onset of depletion to higher signal power levels.

3. Experiment results

The response of a tunable optical filter based on the vector properties of SBS was measured experimentally. The measurement setup is shown in Fig. 2. Light from a distributed feedback (DFB) laser diode was used as an SBS pump wave. The optical spectrum of the pump was broadened through direct modulation of the DFB injection current, using the output of an arbitrary waveform generator (see Fig. 3) [7]. Figure 4 shows a heterodyne measurement of the pump PSD, taken through beating of the pump wave with a detuned local oscillator on a broadband detector. The 700 MHz-wide pump wave was amplified to a power level of 13.5 dBm by an Erbium-doped fiber amplifier (EDFA), and launched into a 3.5 km-long, highly nonlinear fiber under test (FUT) via a circulator. The fiber length and SBS gain coefficient, as well as the pump power, matched those of the simulation of the previous section. A 1.5 nm-wide optical band-pass filter was used to reduce the ASE of the EDFA.

#152142 - $15.00 USD Received 1 Aug 2011; revised 31 Aug 2011; accepted 1 Sep 2011; published 21 Oct 2011

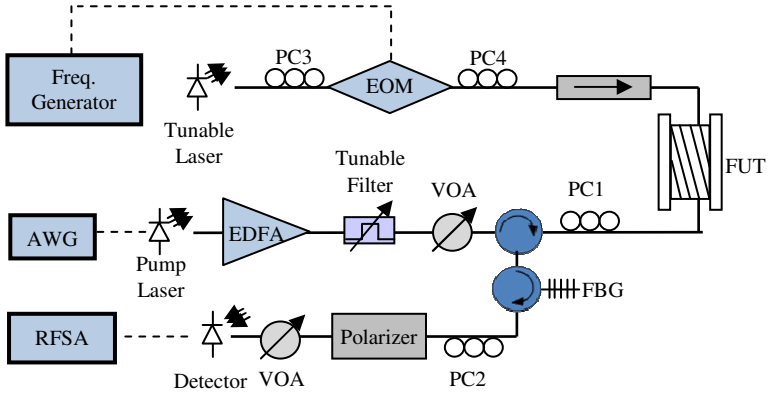

Fig. 2. Experimental setup for measuring the power transfer function of a polarization-enhanced SBS filter. The SBS signal wave is generated at the upper branch, using a tunable laser that is externally modulated. The electro-optic modulator (EOM) is driven by a radio-frequency tone in the range of 13.5-16.5 GHz, which in turn was amplitude-modulated by a 1 MHz sine wave. The optical polarization was adjusted by polarization controllers (PC). The signal was launched into the fiber under test (FUT) through an isolator. The middle branch is used to realize a 0.7 GHz broadband pump wave, through the direct modulation of a DFB laser by a properly programmed arbitrary waveform generator (AWG). The pump power is amplified and adjusted to 13.5 dBm by an EDFA and a Variable Optical Attenuator (VOA), and directed into the FUT by a circulator. The lower branch includes a 5 GHz-wide FBG for selecting a single sideband of the signal wave, an output polarizer and a photo-detector. The detected signal was analyzed by a radio frequency spectrum analyzer (RFSA).

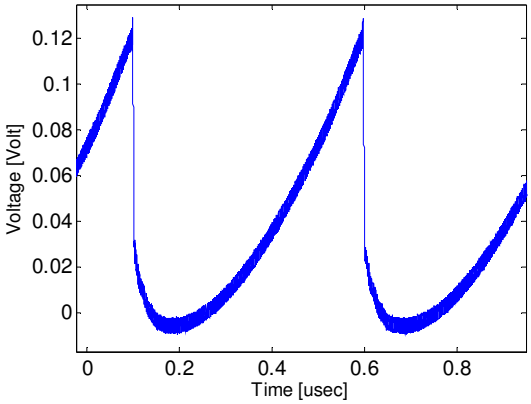

Fig. 3. The direct current modulation waveform used in the spectral broadening of the SBS pump wave.

#152142 - $15.00 USD Received 1 Aug 2011; revised 31 Aug 2011; accepted 1 Sep 2011; published 21 Oct 2011

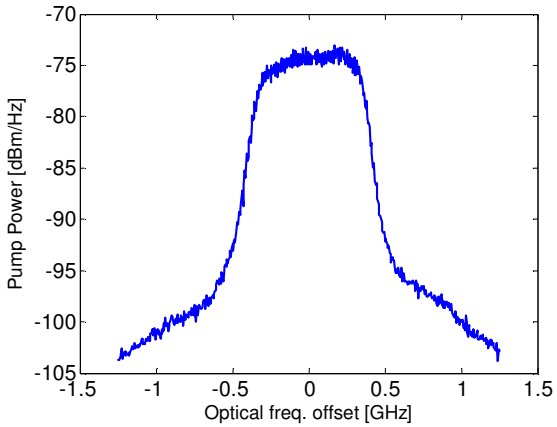

Fig. 4. Measured PSD of the pump wave, as a function of the offset from its central frequency.

Light from a tunable laser diode was used to generate the SBS signal wave. The laser output was double-sideband modulated using a $LiNbO_3$ Mach-Zehnder interferometer (Electro-Optical Modulator – EOM), driven by a swept sine wave of frequency Ω_{RF}, in the range of $2\pi\cdot13.5$-$2\pi\cdot16.5$ GHz. The tunable laser carrier wavelength and the radio-frequency (RF) modulation were chosen so that one of the sidebands scanned the SBS amplification spectral window that was induced by the pump wave, as in Fig. 5. The modulated signal wave was launched into the FUT from the end opposite to that of the pump input. Following propagation through the FUT, the signal was filtered by a 5 GHz-wide fiber Bragg grating (FBG), which retained only the side-band of interest and blocked off the carrier wavelength, Rayleigh back-scatter of the pump wave and the other sideband. Lastly, the signal passed through a Polarization controller (PC) and a linear polarizer. The filtered signal power at the polarizer output was observed directly by a 125 MHz-wide photo-detector. In order to distinguish between the signal the induced SBS-ASE, the RF sine wave at Ω_{RF} was further amplitude modulated by a 1-MHz tone, and the detector output power was measured by an RF spectrum analyzer (RFSA), using zero-span at 1MHz with a resolution bandwidth of 100Hz.

#152142 - $15.00 USD Received 1 Aug 2011; revised 31 Aug 2011; accepted 1 Sep 2011; published 21 Oct 2011

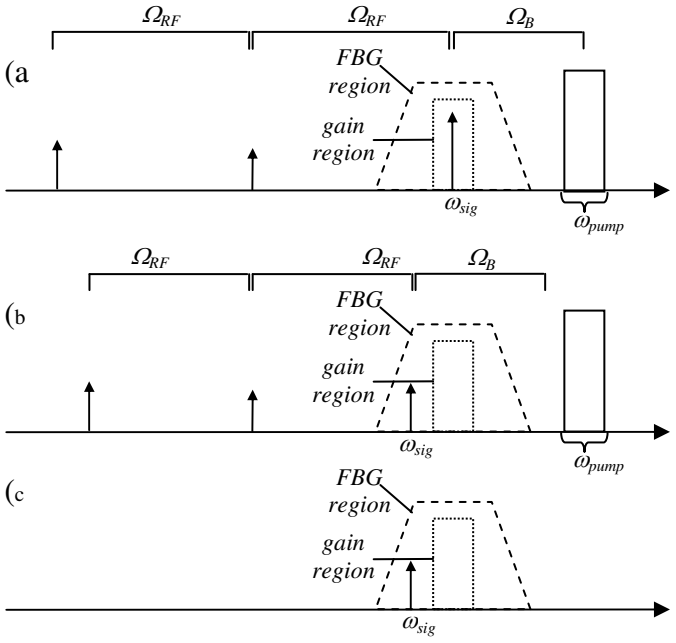

Fig. 5. The generation of the SBS signal wave. (a-b): Schematic spectrum of double-sideband modulated tunable laser. The radio-frequency (RF) modulation waveform is a swept sine-wave Ω_{RF} in the $2\pi\cdot13.5$ to $2\pi\cdot16.5$ GHz range. Depending on Ω_{RF}, the upper modulation sideband could fall within the SBS amplification spectral region induced by the pump (a), or outside that region (b). (c): Spectrum of signal wave following propagation in the FUT and after filtering by a 5 GHz-wide FBG, which retains the upper modulation sideband only. The additional 1MHz amplitude modulation of the carrier is not shown.

First, the optical power transmission of a scalar SBS-based filter without polarization discrimination was characterized (as in [7]). In this set of measurements, the output polarizer was removed, and the input SOP of the signal was adjusted using PC4 for maximum amplification. The carrier frequency of the tunable laser was set to 15 GHz below the center of the SBS amplification band, as induced by the pump wave. Figure 6 shows the measured optical power gain of the sideband of interest as a function of Ω_{RF}, which was scanned around $2\pi\cdot15$GHz. Measurements were taken for several signal power levels in the range of −18.1 to 2.7 dBm. A maximum selectivity of 22 dB was achieved in the undepleted pump regime. Pump depletion reduces the filter selectivity to 12.7 dB when the input signal power is raised to 2.7 dBm.

Figure 7 shows the corresponding signal power gain at the output of a polarization-enhanced filter. In the absence of the input signal, $\hat{e}_{sig}^{out\ \max}$ was first identified as the SOP of SBS-ASE [16]. Then, using PC1, $\hat{e}_{sig}^{out\ \max}$ was oriented at 45° with respect to the output polarizer (i.e. $p_{\max,\min}=\pm1/\sqrt{2}$), as discussed in the previous section. Finally, PC4 was readjusted for maximum rejection of the unamplified signal components, thereby implementing $a=b=1/\sqrt{2}$. Using the polarization enhanced configuration, the filter selectivity for the higher optical signal power level of −3.1 dBm was improved considerably, from 16.5 dB to 30 dB. The depletion tolerance of the filter was improved as well: the same frequency response was obtained for signal power levels of −13.1 dBm and −3.1 dBm (see Fig. 7). The power gain within the pass-band of the polarization enhanced filter was 8 dB lower than $|G_{\max}|^2$, in good agreement with the predictions of Fig. 1.

#152142 - $15.00 USD Received 1 Aug 2011; revised 31 Aug 2011; accepted 1 Sep 2011; published 21 Oct 2011

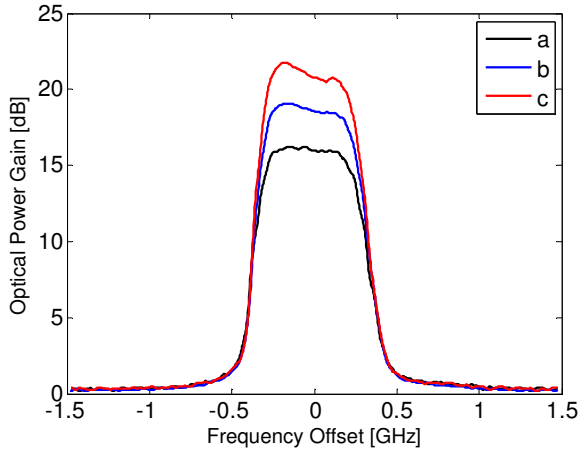

Fig. 6. Relative sideband power gain of a scalar SBS-based filter, without polarization enhancement. Input signal power levels: (a) –3.1 dBm, (b) –8.2 dBm and (c) –13.1 dBm. A 13.5 dBm, 0.7 GHz-wide pump signal was used (Fig. 3).

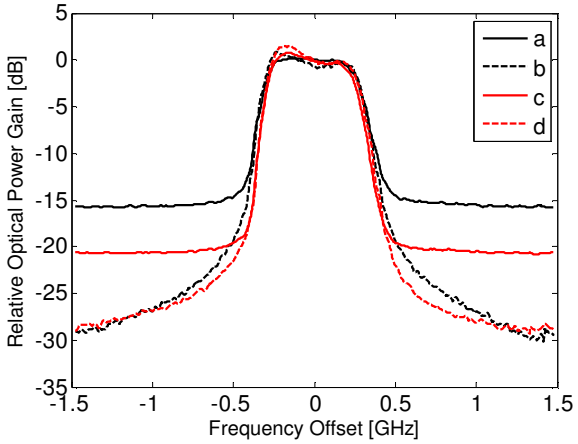

Fig. 7. Comparison between the relative optical power gain of SBS-based tunable bandpass filters without (a, c) and with (b, d) polarization enhancement, using equal pump (13.5 dBm) and signal (–3.1, –13.1 dBm) power levels. Curves (a, c) are identical to Fig. 6(a, c).

4. Discussion

In this work we have demonstrated a significant enhancement in the performance of SBS-based tunable band-pass filters. The improvement relies on the vector properties of the SBS amplification: the output SOP of amplified signal components is pulled towards a specific state, whereas the SOP of unamplified signal components is unaffected by SBS. Polarization-based discrimination, with judicious alignment of the input SOPs, provides an improvement in the filter selectivity in the undepleted pump regime. In addition, the depletion threshold of the filter is elevated as well. Care must be taken, though, in the application of the filter above the depletion threshold, as the transfer of broadband Stokes waves could be different from that of monochromatic signals. The filter bandwidth can be arbitrarily increased (up to ~10GHz [14]) by further pump broadening, at the expense of lower gains and increased vulnerability to PMD. Finally, proper tracking and compensation of slow polarization drifts may be necessary for the stable, long-term operation of the filters [19].

#152142 - $15.00 USD Received 1 Aug 2011; revised 31 Aug 2011; accepted 1 Sep 2011; published 21 Oct 2011

In our experiments a 0.7 GHz-wide, polarization-enhanced filter provided a 30 dB selectivity in amplifying input signals having a range of optical power levels, from −13.1 to −3.1 to dBm. A scalar SBS-based filter, without polarizarion considerations, provided only 22 to 16.5 dB selectivity for the same input power levels of signal and pump. The obtained performance is superior to that of our previous work [7], in which a power gain selectivity of only 14 dB was achieved with a similar pump PSD and using the same fiber. The filter selectivity can be further increased using higher pump power levels [7]. The spectral power transmission of SBS-based tunable filters is very sharp: a 20 dB change in transmission occurs within a 200 MHz-wide spectral region. The central frequeny of the filter can be varied arbitrarily, and its bandwidth can be independently scaled between 30 MHz to ~10 GHz through pump modulation. SBS pump synthesis can further allow for the flexible pre-emphasis and spectral shaping of the filter pass-band.

SBS-based photonic filters could also be highly attractive, for example, in selecting sub-bands of modern coherent optical communication systems, such as optical orthogonal frequency domain multiplexing (O-OFDM) [20]. The proposed technique can also be adapted to microwave-photonic filtering of broadband RF signals. In SBS-based microwave-photonic filters, an optical carrier is single-sideband modulated by the RF signal of interest. The modulation sideband undergoes frequency-selective SBS amplification as described above, and the modified RF waveform is recovered through beating of the sideband with the optical carrier upon detection. The RF power gain of the filter therefore scales with the optical power gain of the modulation sideband. SBS-based RF photonic filters would provide a sharp and aperiodic transfer function, with independently tunable central radio frequency, width and shape. The experimental transfer function obtained in the previous section is analogous to that of a sharp microwave-photonic filter, whose pass-band is centered at 15 GHz. Finally, frequency-selective polarization pulling of SBS amplification was also recently employed in the generation of an advanced modulation format [21].

In conclusion, tunable and sharp optical band-pass filters were proposed and demonstrated, based on the insight that has been provided by the vector analysis of SBS in randomly birefringent fibers.

Acknowledgement

The work of M. Tur and A. Wise was supported in part by the Israeli Science Foundation (ISF).

#152142 - $15.00 USD Received 1 Aug 2011; revised 31 Aug 2011; accepted 1 Sep 2011; published 21 Oct 2011